A rigorous electrochemical ammonia synthesis protocol with quantitative isotope measurements

Andersen, Suzanne Zamany; Čolić, Viktor; Yang, Sungeun; Schwalbe, Jay A.; Nielander, Adam C.; McEnaney, Joshua M.; Enemark-Rasmussen, Kasper; Baker, Jon G.; Singh, Aayush R.; Rohr, Brian A.

Total number of authors:
21

Published in:
Nature

Link to article, DOI:
10.1038/s41586-019-1260-x

Publication date:
2019

Document Version
Peer reviewed version

nature Accelerated Article Preview

LETTER
doi:10.1038/s41586-019-1260-x

A rigorous electrochemical ammonia synthesis protocol with quantitative isotope measurements

Suzanne Z. Andersen, Viktor Čolić, Sungeun Yang, Jay A. Schwalbe, Adam C. Nielander, Joshua M. McEnaney, Kasper Enemark-Rasmussen, Jon G. Baker, Aayush R. Singh, Brian A. Rohr, Michael J. Statt, Sarah J. Blair, Stefano Mezzavilla, Jakob Kibsgaard, Peter C. K. Vesborg, Matteo Cargnello, Stacey F. Bent, Thomas F. Jaramillo, Ifan E. L. Stephens, Jens K. Nørskov & Ib Chorkendorff

Cite this article as: Andersen, S. Z. et al. A rigorous electrochemical ammonia synthesis protocol with quantitative isotope measurements. *Nature* https://doi.org/10.1038/s41586-019-1260-x (2019).

Received: 8 June 2018; Accepted: 9 May 2019;
Accelerated Article Preview Published online 22 May 2019.

LETTER

https://doi.org/10.1038/s41586-019-1260-x

A rigorous electrochemical ammonia synthesis protocol with quantitative isotope measurements

Suzanne Z. Andersen[1,5], Viktor Čolić[1,5], Sungeun Yang[1,5], Jay A. Schwalbe[2], Adam C. Nielander[2], Joshua M. McEnaney[2], Kasper Enemark-Rasmussen[3], Jon G. Baker[2], Aayush R. Singh[2], Brian A. Rohr[2], Michael J. Statt[2], Sarah J. Blair[2], Stefano Mezzavilla[1], Jakob Kibsgaard[1], Peter C. K. Vesborg[1], Matteo Cargnello[2], Stacey F. Bent[2], Thomas F. Jaramillo[2], Ifan E. L. Stephens[4], Jens K. Nørskov[2] & Ib Chorkendorff[1]*

The electrochemical synthesis of ammonia from nitrogen under mild conditions and using renewable electricity is in principle an attractive alternative[1–4] to the demanding, energy-intense Haber–Bosch process, which dominates industrial ammonia production. However, the electrochemical alternative faces considerable scientific and technical challenges[5,6] and most experimental studies reported thus far achieve only low selectivities and conversions. In fact, the amount of ammonia produced is usually so small that it is difficult to firmly attribute it to electrochemical nitrogen fixation[7–9] and exclude contamination due to ammonia that is either present in air, human breath or ion-conducting membranes[9], or generated from labile nitrogen-containing compounds (for example, nitrates, amines, nitrites and nitrogen oxides) that are typically present in the nitrogen gas stream[10], in the atmosphere or even the catalyst itself. Although these many and varied sources of potential experimental artefacts are beginning to be recognized and dealt with[11,12], concerted efforts to develop effective electrochemical nitrogen reduction processes would benefit from benchmarking protocols for the reaction and from a standardized set of control experiments to identify and then eliminate or quantify contamination sources. Here we put forward such a rigorous procedure that, by making essential use of $^{15}N_2$, allows us to reliably detect and quantify the electroreduction of N_2 to NH_3. We demonstrate experimentally the significance of various sources of contamination and show how to remove labile nitrogen-containing compounds present in the N_2 gas and how to perform quantitative isotope measurements with cycling of $^{15}N_2$ gas to reduce both contamination and the cost of isotope measurements. Following this protocol, we obtain negative results when using the most promising pure metal catalysts in aqueous media, and successfully confirm and quantify ammonia synthesis using lithium electrodeposition in tetrahydrofuran[13].

Ru, Re and Rh are the most promising pure metal catalysts[14], for which our electrochemical benchmarking experiments in aqueous electrolyte did not yield more ammonia than the background level of ~10 ppb (Fig. 1). We conclude that under these conditions no ammonia is synthesized, and that the competing hydrogen evolution reaction (HER) dominates in an aqueous environment[5]. Figure 2A-C compare the ammonia levels seen in this negative result experiment with levels reported in the literature, illustrating that reported ammonia production rates and concentrations are often close to common background levels that we also explicitly quantify (see Extended Data Figure 1). Reporting only ammonia production rates, without careful control experiments, is thus clearly not sufficient to reliably document ammonia formation. The problem of spurious nitrogen[15] giving rise to experimental artefacts is well recognized in other fields, and likely explains the inability to reproduce[16] photochemical NH_3 synthesis over TiO_2 under rigorous conditions. This difficulty is also increasingly recognized in the context of electrochemical ammonia synthesis, where recent re-testing of a putative phthalocyanine-based ammonia electrosynthesis catalyst attributed detected ammonia to contaminants or catalyst decomposition[17] and measurement protocol are being developed to ensure false positives are distinguished from breakthrough results[11,12].

As noted by others when discussing the need to improve on how ammonia measurements and controls are conducted[11,12], a range of factors need to be considered to ensure detected ammonia has been produced from dinitrogen rather than adventitious contamination. To this end, we implement a systematic benchmarking protocol that also quantifies N_2 electroduction and is presented in Fig. 3 in flow chart form.

As noted by others[11,12], an essential first control is performing measurements with Ar under the exact same conditions as the N_2 electroreduction experiments to quantify ammonia originating from contamination within the cell or the catalyst itself. A control with N_2 at open circuit potential (OCP) over the same duration as the electroreduction experiment is equally important, to explore contamination in the feed gas stream. We note, however, that even high purity N_2 gas can contain in addition to ammonia itself also easily reduced nitrogen sources such as NO_x, so nitrogen gas as a source of adventitious contamination should be dealt with by first passing it over an appropriate adsorbent, e.g. Cu (see Methods section).

Other sources of contamination may also be present and result in activity tests yielding a comparable level of ammonia to control tests. These sources include Nafion, which is employed in some N_2 electroreduction experiments as a separating membrane or electrolyte[9,18] and which accumulates and releases NH_4^+ through ion exchange with acid groups (see Methods section). Ambient air also contains a non negligible amount of ammonia (ranging from 0.05-250 ppm[19]) that can accummulate in chemicals and/or the experimental setup, making use of a closed system therefore imperative. Similarly, human breath contains 0.3-3.0 ppm ammonia[20] and needs to be carefully excluded. The presence and strength of these sources of contamination vary enonrmously, so persuasive evidence for successful electrochemical ammonia synthesis requires the accumulation of ammonia in concentrations significantly exceeding the concentration obtained in control measurements with Ar as well as N_2 at OCP over the same duration.

More definite proof that measured ammonia originates from N_2 electroreduction calls for experiments using isotopically labelled $^{15}N_2$ gas and detection of the $^{15}NH_3$ produced with an isotope sensitive method. In this control, the amount of $^{15}NH_3$ produced should be in quantitative agreement with the amount of $^{14}NH_3$ produced in the equivalent $^{14}N_2$ reduction tests. We note here that although recent studies included in Fig. 2 include isotope labelling experiments, most lack quantitative data and would fail the requirements of our protocol.

Methods such as mass spectroscopy[21] and IR measurements[22] can discriminate $^{15}NH_3$ from $^{14}NH_3$ (see Methods section and Extended

[1]Department of Physics, Technical University of Denmark, Kgs, Lyngby, Denmark. [2]SUNCAT Center for Interface Science and Catalysis, Department of Chemical Engineering, Stanford University, Stanford, CA, USA. [3]Department of Chemistry, Technical University of Denmark, Kgs, Lyngby, Denmark. [4]Department of Materials, Imperial College London, London, UK. [5]These authors contributed equally: Suzanne Z. Andersen, Viktor Čolić, Sungeun Yang. *e-mail: Ibchork@fysik.dtu.dk

Data Figure 3), with our focus here on NMR which we found most convenient. ^{1}H NMR can differentiate the isotopes, as the scalar interaction between ^{1}H and ^{15}N in $^{15}NH_4^+$ results in a splitting of the ^{1}H resonance into two symmetric signals with a spacing of 73 Hz, while the ^{1}H resonance coupled to ^{14}N in $^{14}NH_4^+$ is split into three symmetric signals with a spacing of 52 Hz. A solution with no added ammonia still shows faint peaks for $^{14}NH_4^+$, due to the aforementioned background contamination. The peaks for $^{15}NH_4^+$ are distinguishable at concentrations down to 51 ppb under the conditions described in the Methods section using an 800 MHz NMR instrument, and the amounts of $^{14}NH_4^+$ and $^{15}NH_4^+$ can be quantified from the integrated areas. We have also demonstrated this strategy using a lower field and more common 400 MHz NMR system (see Extended Data Figure 2).

Isotope labelled $^{15}N_2$ gas usually contains not only ammonia as an imputity, but also reducible labile nitrogen containing compounds such as NO_x[10]. As an illustration of the potential impact of such impurities, consider a recent study reporting μg NH_3 yields obtained through electroreduction of a very small fraction of the nitrogen reactant gas over the course of several days[23]. The isotope labelling control in the study used $^{15}N_2$ gas with a purity of 99.13%, bubbled for 28 hours at a rate of 10 ml/min – with the 0.87% of impurities potentially leading to 3,600 μg of ammonia or other nitrogen-containing species per hour, which over the course of the experiment would equate to 100 mg and vastly exceed the reported ammonia yield. This illustrates the great care that needs to be taken when dealing with the almost inevitable contamination of the nitrogen gas, as even impurity levels restrictied to a few ppm can be highly problematic. Although control measurements with $^{15}N_2$ gas flowing through the cell under OCP must be conducted to establish the level of ammonia contamination from the gas feed, in the same manner as measurements with $^{14}N_2$ gas, additional purification is essential before the gas enters the electrochemical cell. This can be effectively achieved through adsorption on a reduced copper catalyst (see Methods section). We have implemented this using a gas recycling set-up (see Methods), which allows us to lower impurity levels and reuse expensive $^{15}N_2$ when conducting istope labelling control experiments.

When electroreduction of nitrogen to ammonia is successfully observed, experiments will need to be repeated to establish reproducible results with error bars, and so that mean and variance of the data can be determined. To enable meaningful comparison of data collected under different conditions in different experimental setups, we suggest reporting the actual concentration of detected ammonia, the concentrations measured in control measurements and the electrolyte volume. Useful figures-of-merit that should be reported include the partial current density for ammonia synthesis, in mA/cm^2 and normalised to geometric and electrochemically active surface area; turnover frequency (TOF) per site per second; working electrode potential; Faradaic efficiency; yield rate normalized to electrode surface area and catalyst mass. The amount of ammonia produced can be quantified using isotope specific NMR and colorimetric measurements (see Methods), which must give similar results. Importantly, there must also be a 1:1 agreement between the amounts of ammonia produced in the $^{14}N_2$ and $^{15}N_2$ reduction tests performed under the same conditions.

We have used our proposed protocol to test several of the more promising processes and catalysts shown in Fig. 2, but have so far only been able to reproduce the lithium-mediated nitrogen electroreduction experiment[24] that measured high current densities and determined ammonia concentrations using a colorimetric indophenol test and an ammonia gas sensing electrode. While the original study lacked crucial isotope labelled measurements, we were able to confirm NH_3 formation using a molybdenum foil and $^{14}N_2$ gas by determing $^{14}NH_3$ with a colorimetric method and with NMR (Fig. 4A,B). Contols with Ar accumulating 20 C of charge and $^{14}N_2$ gas at OCP for 1.5 hours gave no discernible amount of NH_3. Final ammonia electrosynthesis experiments using isotopically labelled $^{15}N_2$ (containing 2% $^{14}N_2$, with the gas cleaned using Cu catalyst as an impurity trap; see Methods section) confirmed electrochemical production of $^{15}NH_3$ from $^{15}N_2$ (Fig. 4C), with the amount of accumulated ammonia correlated with the amount of charge passed through the system (Fig. 4D). When using $^{14}N_2$ gas, ammonia quantification using NMR and indophenol measurements gave a mean Faradaic efficiency of, respectively, 6.5±1.4% and 7.5±1.1%; a mean yield rate of 0.7±0.2 μmol/h·cm^2 and 0.8±0.1 μmol/h·cm^2, respectively; and a mean concentration after 20 C of charge had passed of 0.56±0.10 mM (9.6±1.6 ppm) and 0.65±0.08 mM (11.1±1.3 ppm), respectively. When using $^{15}N_2$ gas, ammonia determined by NMR and indophenol measurements gave a mean faradaic efficiency of, respectively, 5.7±0.7% and 7.0±2.2%; and mean yield rate of 0.6±0.1 μmol/h·cm^2 and 0.7±0.2 μmol/h·cm^2, respectively; and a mean concentration after 20 C charge had passed of 0.49±0.05 mM (8.3±0.9 ppm) and 0.61±0.16 mM (10.3±2.7 ppm), respectively. While the exact nature of the ammonia synthesis will be the subject of a future report, our observations validate the lithium-mediated strategy for electrochemical NH_3 production ammonia and illustrate both that ammonia can be synthesized in similar quantities from $^{14}N_2$ and $^{15}N_2$ and the use of our benchmarking protocol.

We anticipate that our rigorous protocol will enable a more effective identification of electrochemical systems capable of reducting N_2 to NH_3 and, by preventing false positives from appearing in the literature, ultimately aid the development of more efficient processes yielding significantly larger amounts of ammonia than are currently achieved. Once ammonia can be produced at concentrations beyond the ppm range, rigorous protocols with quantitative isotope sensitive experiments may no longer be necessary for every measurement. However, the varied sources of potential contamination will remain and our suggested control experiments thus remain important and relevant when exploring nitrogen conversion processes (including photoelectrochemical reduction and nitrogen oxidation to NO_x).

Online content

Any methods, additional references, Nature Research reporting summaries, source data, statements of data availability and associated accession codes are available at https://doi.org/10.1038/s41586-019-1260-x.

Received: 8 June 2018; Accepted: 9 May 2019;
Published online 22 May 2019.

1. Shipman, M. A. & Symes, M. D. Recent progress towards the electrosynthesis of ammonia from sustainable resources. *Catal. Today* **286**, 57–68 (2017).
2. Jewess, M. & Crabtree, R. H. Electrocatalytic Nitrogen Fixation for Distributed Fertilizer Production? *ACS Sustain. Chem. Eng.* **4**, 5855–5858 (2016).
3. Nørskov, J., Chen, J. DOE Roundtable Report: Sustainable Ammonia Synthesis. *U.S. Dep. Energy* (2016).
4. Ye, L., Nayak-Luke, R., Bañares-Alcántara, R. & Tsang, E. Reaction: "Green" Ammonia Production. *Chem* **3**, 712–714 (2017).
5. Singh, A. R. *et al.* Electrochemical Ammonia Synthesis—The Selectivity Challenge. *ACS Catal.* **7**, 706–709 (2017).
6. Skúlason, E. *et al.* A theoretical evaluation of possible transition metal electro-catalysts for N_2 reduction. *Phys. Chem. Chem. Phys.* **14**, 1235–1245 (2012).
7. Sclafani, A., Augugliaro, V., Schiavello, M. Dinitrogen Electrochemical Reduction to Ammonia over Iron Cathode in Aqueous Medium. *J. Electrochem. Soc.* **130**, 734 (1983).
8. Zhang, Z., Zhong, Z. & Liu, R. Cathode catalysis performance of $SmBaCuMO_{5+\delta}$ (M=Fe, Co, Ni) in ammonia synthesis. *J. Rare Earths* **28**, 556–559 (2010).
9. Lan, R., Irvine, J. T. S. & Tao, S. Synthesis of ammonia directly from air and water at ambient temperature and pressure. *Sci. Rep.* **3**, 1145 (2013).
10. Dabundo, R. *et al.* The Contamination of Commercial $^{15}N_2$ Gas Stocks with ^{15}N–Labeled Nitrate and Ammonium and Consequences for Nitrogen Fixation Measurements. *PLoS One* **9**, e110335 (2014).
11. Greenlee, L. F., Renner, J. N. & Foster, S. L. The Use of Controls for Consistent and Accurate Measurements of Electrocatalytic Ammonia Synthesis from Dinitrogen. *ACS Catal.* **8**, 7820–7827 (2018).
12. Chen, G.-F. *et al.* Advances in Electrocatalytic N_2 Reduction-Strategies to Tackle the Selectivity Challenge. *Small Methods* **1800337**, 1800337 (2018).
13. Tsuneto, A., Kudo, A. & Sakata, T. Efficient Electrochemical Reduction of N_2 to NH_3 Catalyzed by Lithium. *Chem. Lett.* **22**, 851–854 (1993).
14. Montoya, J. H., Tsai, C., Vojvodic, A. & Nørskov, J. K. The Challenge of Electrochemical Ammonia Synthesis: A New Perspective on the Role of Nitrogen Scaling Relations. *ChemSusChem* **8**, 2180–2186 (2015).
15. Hager, T. *The Alchemy of Air*. (Harmony Books, 2008).

16. Boucher, D. L., Davies, J. A., Edwards, J. G. & Mennad, A. An investigation of the putative photosynthesis of ammonia on iron-doped titania and other metal oxides. *J. Photochem. Photobiol. A Chem.* **88**, 53–64 (1995).
17. Shipman, M. A. & Symes, M. D. A re-evaluation of Sn(II) phthalocyanine as a catalyst for the electrosynthesis of ammonia. *Electrochim. Acta* **258**, 618–622 (2017).
18. Shi, M.-M. *et al*. Au Sub-Nanoclusters on TiO_2 toward Highly Efficient and Selective Electrocatalyst for N_2 Conversion to NH_3 at Ambient Conditions. *Adv. Mater.* **29**, 1606550 (2017).
19. Schlesinger, W. & Hartley, A. A global budget for atmospheric NH_3. *Biogeochemistry* **15**, 191–211 (1992).
20. Turner, C., Španěl, P. & Smith, D. A longitudinal study of ammonia, acetone and propanol in the exhaled breath of 30 subjects using selected ion flow tube mass spectrometry, SIFT-MS. *Physiol. Meas.* **27**, 321–337 (2006).
21. Song, Y. *et al*. A physical catalyst for the electrolysis of nitrogen to ammonia. *Sci. Adv.* **4**, e1700336 (2018).
22. McEnaney, J. M. *et al*. Ammonia synthesis from N_2 and H_2O using a lithium cycling electrification strategy at atmospheric pressure. *Energy Environ. Sci.* **10**, 1621–1630 (2017).
23. Wang, H. *et al*. Ambient Electrosynthesis of Ammonia: Electrode Porosity and Composition Engineering. *Angew. Chemie Int. Ed.* **57**, 12360–12364 (2018).
24. Tsuneto, A., Kudo, A. & Sakata, T. Lithium-mediated electrochemical reduction of high pressure N_2 to NH_3. *J. Electroanal. Chem.* **367**, 183–188 (1994).
25. Bao, D. *et al*. Electrochemical Reduction of N_2 under Ambient Conditions for Artificial N_2 Fixation and Renewable Energy Storage Using N_2 /NH_3 Cycle. *Adv. Mater.* **29**, 1604799 (2017).
26. Chen, G.-F. *et al*. Ammonia Electrosynthesis with High Selectivity under Ambient Conditions via a Li^+ Incorporation Strategy. *J. Am. Chem. Soc.* **139**, 9771–9774 (2017).
27. Kong, J. *et al*. Electrochemical Synthesis of NH_3 at Low Temperature and Atmospheric Pressure Using a γ-Fe_2O_3 Catalyst. *ACS Sustain. Chem. Eng.* **5**, 10986–10995 (2017).
28. Yao, Y., Zhu, S., Wang, H., Li, H. & Shao, M. A Spectroscopic Study on the Nitrogen Electrochemical Reduction Reaction on Gold and Platinum Surfaces. *J. Am. Chem. Soc.* **140**, 1496–1501 (2018).
29. Kim, K., Yoo, C.-Y., Kim, J.-N., Yoon, H. C. & Han, J.-I. Electrochemical Synthesis of Ammonia from Water and Nitrogen in Ethylenediamine under Ambient Temperature and Pressure. *J. Electrochem. Soc.* **163**, F1523–F1526 (2016).
30. Zhou, F. *et al*. Electro-synthesis of ammonia from nitrogen at ambient temperature and pressure in ionic liquids. *Energy Environ. Sci.* **10**, 2516–2520 (2017).

Acknowledgements This work was supported by the Villum Foundation V-SUSTAIN grant 9455 to the Villum Center for the Science of Sustainable Fuels and Chemicals. 400 MHz and 800 MHz NMR spectra were recorded on the spectrometers of the NMR Center at DTU supported by the Villum Foundation. We acknowledge Albert Kravos' contribution in setting up the analytical methods to detect ammonia.

Reviewer information *Nature* thanks Lauren Greenlee, Mark Symes and the other anonymous reviewer(s) for their contribution to the peer review of this work.

Author contributions S.Z.A., V.C., S.Y., J.K., S.M., P.C.K.V., I.E.L.S., and I.C. concieved the idea for the protocol and experiment design. S.Z.A., V.C., S.M. and S.Y., performed the experiments, V.C. performed potential scale determination and iR-drop correction, S.Y. performed isotope measurements, K.E.-R. performed NMR measurements and wrote NMR section, J.S., A.C.N., and J.M.M. performed FTIR measurements and wrote FTIR section, J.K., P.C.K.V., I.E.L.S., and I.C. supervised the work, S.Z.A., V.C., and S.Y. drafted the manuscript, and all authors contributed to the editing of the manuscript.

Competing interests The authors declare no competing interests.

Additional information
Extended data is available for this paper at https://doi.org/10.1038/s41586-019-1260-x.
Reprints and permissions information is available at http://www.nature.com/reprints.
Correspondence and requests for materials should be addressed to I.C.
Publisher's note: Springer Nature remains neutral with regard to jurisdictional claims in published maps and institutional affiliations.

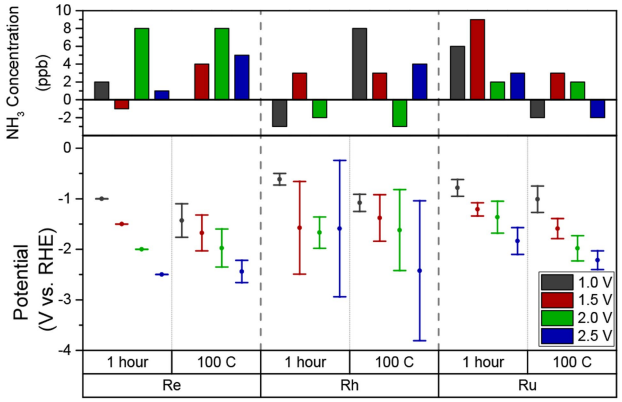

Fig. 1 | Potential range for chronoamperometric measurements (below) of pure metal catalysts and the detected amounts of ammonia in each measurement (above). Each catalyst was tested both for 1 hour and by passing 100 C of charge at -1.0, -1.5, -2.0 and -2.5 V vs RHE, where the error bars represent a change in potential during the measurement due to a changing ohmic drop correction (see Methods section).

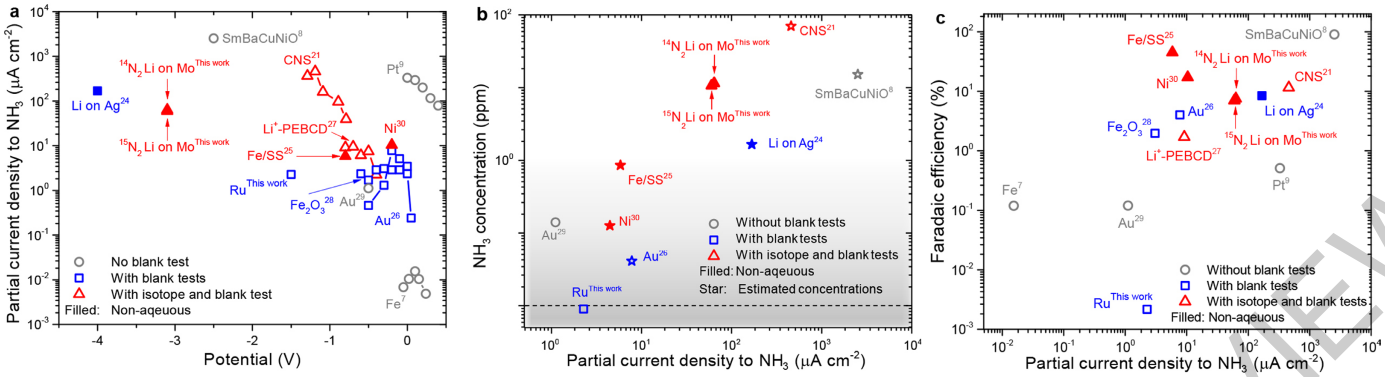

Fig. 2 | An overview on literature data collected in Extended Data Tables 1-4. Grey dots represent data without blank test, blue squares includes blank tests, red triangles represent data with $^{15}N_2$ isotope tests with blank tests, filled symbols signify non-aqueous systems, and stars are estimated values using data provided in the literature. **a** Partial current densities for electrochemical ammonia production vs. applied potential (vs. RHE unless otherwise specified). **b** Ammonia concentrations as a function of partial current density towards ammonia formation. The 10 ppb dashed line signifies the lower detection limit of ammonia in our system, and the grey gradient signifies concentrations wherein we have seen false positives (see Extended Data). **c** Faradaic efficiency of the detected ammonia as a function of partial current density towards ammonia. Data adapted from: Ref[7] for Fe; Ref[8] for SmBaCuNiO; Ref[9] for Pt; Ref[25] for Au; Ref[26] for Li^+-PEBCD (Li^+ incorporated into poly(N-ethyl-benzene-1,2,4,5-tetracarboxylic diimide)); Ref[27] for Fe_2O_3; Ref[28] for Au; Ref[29] for Ni with a potential of 1.8 V between 2 electrodes; Ref[30] for Fe/SS with a potential vs. NHE; Ref[21] for CNS; Ref[24] for Li on Ag with a potential vs. Ag/AgCl/AgCl (sat), LiCl, $LiClO_4$/THF reference. The potential for Li on Mo in this work is -3.1 V vs. SHE.

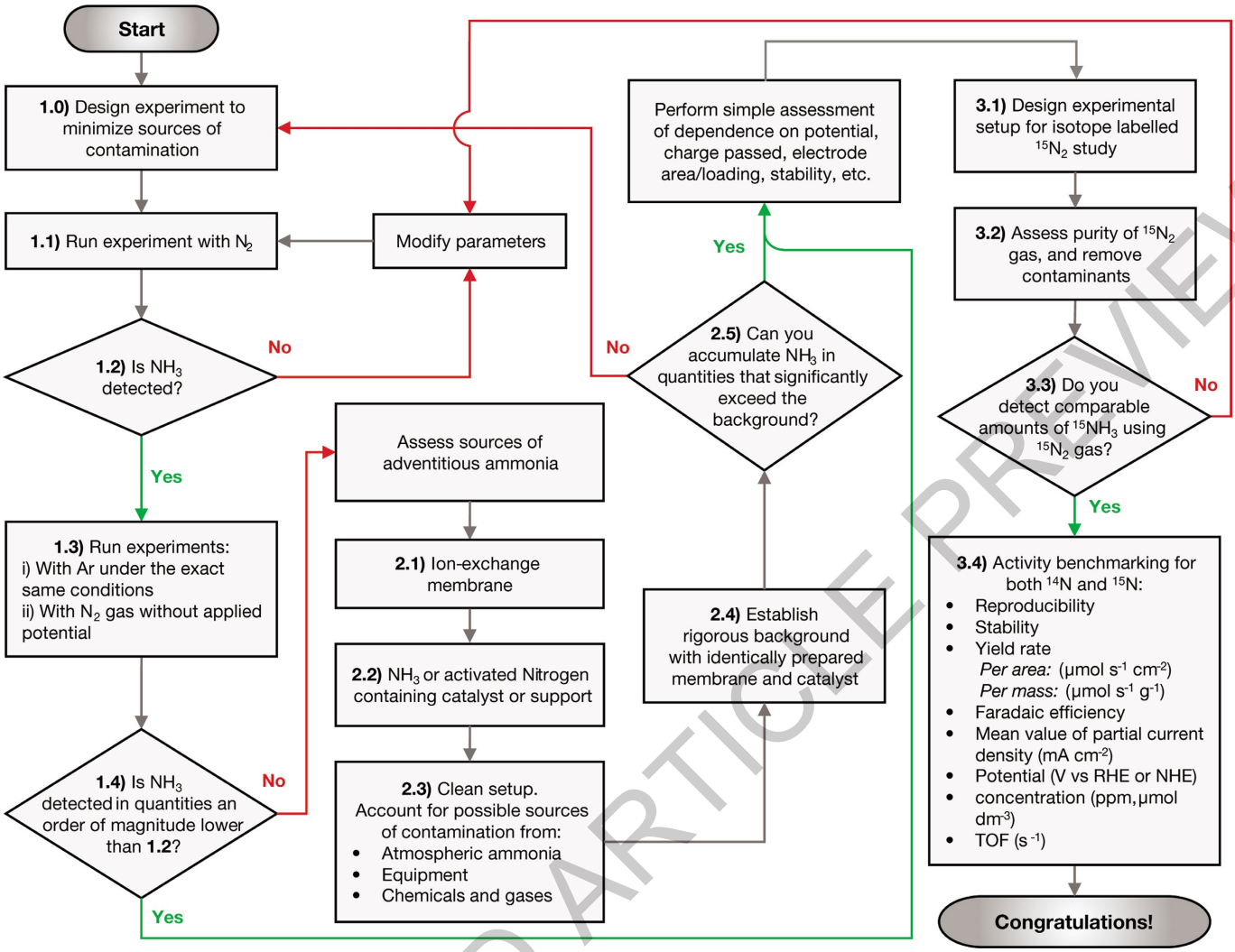

Fig. 3 | Suggested protocol for the benchmarking of electrochemical nitrogen reduction.

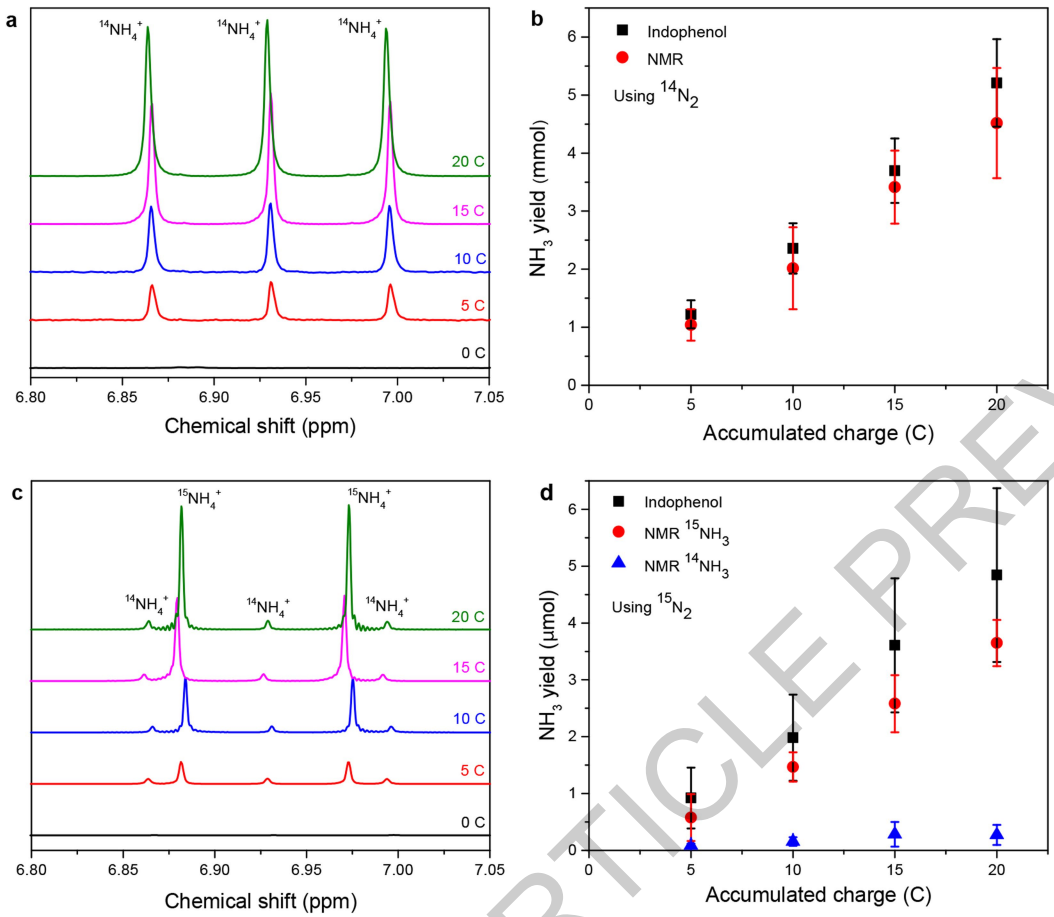

Fig. 4 | Ammonia synthesised at -3.1 V and more negative potentials vs SHE (iR-drop corrected) using a Mo-cathode and Pt-anode in a 0.2 M $LiClO_4$ in 1% ethanol and 99% THF electrolyte, in the system reported by Tsuneto et al., here successfully proven by repeated regular and isotope labelled experiments. a Representative NMR data of experiment with samples taken at 5 C, 10 C, 15 C, and 20 C using $^{14}N_2$ with THF suppression (for details see Methods section), and b mean and standard deviation of 3 measurements of $^{14}NH_3$ synthesized via integrated peak area from NMR data calibrated with Extended Data Figure 2B-C and indophenol. c Representative NMR data of experiment with $^{15}N_2$, with samples taken at 5 C, 10 C, 15 C, and 20 C, and d mean and standard deviation of 3 measurements of $^{15}NH_3$ synthesized via integrated peak area from NMR data calibrated with Extended Data Figure 2C-D and indophenol. The 1H spectra have been referenced setting the chemical shift of the methyl resonance from ethanol to 1.15 ppm (TMS = 0.0 ppm). Shift of NMR peaks due to slight differences in pH, volume, and/or temperature of samples.

METHODS

Electrochemical measurements in aqueous electrolyte. Bio-Logic VMP2 and SP-300 (Bio-Logic, France) potentiostats were used for all electrochemical experiments. A borosilicate glass H-cell was used, with working electrode (WE) and counter electrode (CE) chambers each 7.5 ml in volume, connected by a joint separated by a membrane. The Hg-Hg_2SO_4 reference electrode (SI Analytics, Germany) reference electrode (RE) chamber is connected to the WE compartment by a glass frit. The electrolyte used is 0.1 M KOH (99.995%, Merck Suprapur®, Germany) in ultrapure water (Millipore Synergy® UV). The glassware is boiled and rinsed twice in Millipore water, then oven dried overnight at 120 °C between each measurement. We use the microporous polypropylene Celgard® 3401 membrane, with a thickness of 25 μm and a porosity of 41% to separate WE and CE chambers. Because it is a porous membrane, as opposed to a proton or anion exchange membrane, it does not act as a source or sink for ammonia, requires no cleaning procedure, and can be kept in 0.1 M KOH. Ruthenium (6×6×1 mm^3, 99.9%, Goodfellow Inc., Canada), rhenium (10×10×2 mm^3, 99.99%, Goodfellow Inc., Canada), and rhodium (5×10×0.25 mm^3, 99.9% purity, MaTeCK, Juelich, Germany), were tested at 4 different potentials: -1.0 V, -1.5 V, -2.0 V, and -2.5 V vs. RHE, for 1 hour, or until 100 C of charge was accumulated. The CE was an iridium foil (25×25×0.125 mm^3, 99.9%, Goodfellow inc., Canada). The electrodes are polished several times using polycrystalline diamond paste (Buehler, USA) respectively of sizes 3 μm, 1 μm, and 0.25 μm, until the surface has a mirror finish, followed by an ultra-sonication process in Millipore water and isopropanol (≥ 99.8%, Merck, Germany) between each polishing step, to dislodge any remaining diamond particles. The WE's were annealed at 700-800 °C by induction heating with Ar/5%-H_2 (AGA Gas AB, Sweden) atmosphere for 5 minutes. Given the generally low Faradaic efficiencies observed for nitrogen reduction in the literature, we applied relatively high currents (10-50 mA) to maximise the ammonia in the system. The Ohmic resistance was measured at OCP, by conducting EIS spectra from 30 kHz to 1 Hz before and after each measurement, fitted using EC-Lab V11.02. A shunt capacitance of 2 μF was connected between the RE and CE to eliminate high-frequency artefacts. Bubble formation during the measurement would result in additional uncorrected Ohmic drops. The EIS spectra were fitted using the software to determine the uncompensated resistance. The iR-drop correction was carried out taking into account the current flowing at the given potential. Measurements were conducted with an 85% *iR*-drop automatic compensation, based on the pre-test resistance; the remaining 15% *iR*-drop was corrected a posterior. The pre-test Ohmic drop was higher than the post-test value, due to rising electrolyte levels in the WE compartment and temperature increases; we thus represent the potential as a range of values to account for this change in potentials. Additionally, when we attempted to measure the Ohmic drop in operando, we measured additional at least 6% increase relative to the OCP, due to bubble formation;[31] typically such in operando measurements were impractical, due to the potentiostat overloading. Thus, in order to account for uncertainty in the Ohmic drop, we represent it is a range of values, rather than a discrete datapoint. The higher hydrogen evolution activity of Rh at very negative potentials resulted in particularly large difference between the pre-test and post-test Ohmic drop value, manifested as a large uncertainty in potential.

Figure 1 displays the potential measured for each metal during CA. All of the pure metal catalysts resulted in <10 ppb NH_3, detected via the colorimetric indophenol method at the measured potentials, within the levels of background contamination of the setup. These catalysts show much higher selectivity towards the competing HER in aqueous solutions, consistent with DFT-based models[14].

Electrochemical measurements in non-aqueous electrolyte. The experiments were performed in an OMNI-LAB (Vacuum Atmospheres Co., USA) glovebox and a home-made closed system with N_2 gas recirculation. The single compartment borosilicate glass cell had an electrolyte volume of 8 ml. It had a two-electrode configuration with a Mo foil (0.125 mm, 99.9%, Goodfellow, UK) WE and a Pt-mesh (99.9%, Goodfellow, UK) CE. Experiments in non-aqueous electrolytes were conducted in 0.2 M $LiClO_4$ (battery grade, 99.99%, Sigma Aldrich, Germany) in a mixture of 1 vol.% ethanol (99.5%, AcroSeal®, Sigma Aldrich, Germany) and 99 vol.% tetrahydrofuran (THF, anhydrous, 99.9%, inhibitor-free, Sigma Aldrich). The exact potential vs. SHE was difficult to determine due to the large Ohmic drop and fluctuating current. It was estimated in a three-electrode system using a Ag/Ag^+ electrode prepared by immersing a silver wire (Dansk Hollandsk Ædelmetal, Denmark) in a 0.1 M $AgClO_4$ (Sigma Aldrich, Denmark) in THF, separated from the main chamber with a P4 glass frit. The potential of this electrode was calculated to be 0.77 V vs. SHE using data from Gritzner[32]. The Ohmic drop was measured by the means of EIS. It was generally in the range of 900-1600 Ω for the 0.2 M solution of $LiClO_4$. For the catalytic tests, a bias of –9 V was applied between the electrodes; the current which was in the range of 2-3 mA. Using this system, we estimate the initial WE potential to be ~-3.1 V under reaction conditions, which became more negative during the experiment.

Colorimetric tests to determine concentration of ammonia, nitrite, and hydrazine. Ammonia in the electrolyte was quantified by the indophenol method, which works well for aqueous electrolytes and can be modified to work for non-aqueous electrolytes. For calibration in aqueous electrolytes, a known concentration of NH_4Cl (99.8%, Merck) was added to 0.1 M KOH, then neutralized by adding 0.5 M H_2SO_4 (Suprapur, Merck, Germany). 500 μl of phenol nitroprusside solution (P6994, Sigma Aldrich) and 500 μl of alkaline hypochlorite solution (A1727, Sigma Aldrich) was then added to 2 ml of the neutralized sample. The solution was incubated for 30 min at room temperature in the dark, and the sample absorbance was analyzed by UV-vis spectrometer (UV-2600, Shimadzu, Japan) from 400 nm to 800 nm. The calibration curve was constructed for ammonia with the following concentrations: blank, 10 ppb, 50 ppb, 100 ppb, 500 ppb, 1 ppm and 2 ppm, and a fitted curve of the absorbance peak of each concentration showed a linear regression with an R-squared value of 0.99965. For the non-aqueous electrolyte (0.2 M $LiClO_4$ in 1% ethanol/99% THF), 20 μl of 4 M HCl (37%, VWR Chemicals, USA) was added to 400 μl of the electrolyte, and the solution was dried at 60 °C for 30 min, evaporating the solvent while leaving ammonia in the form of NH_4Cl salt. The remaining salts were dissolved in 2 ml of Milli-Q H_2O, and the indophenol method proceeded as described for the aqueous case. The calibration curve was constructed for ammonia with the same concentrations as the aqueous case, and a fitted curve of the absorbance peak of each concentration showed a linear regression with an R-squared value of 0.99737. It is imperative to make a blank measurement for every sample using the same batch of chemicals, which ensures no significant contamination of the chemicals.

NO_x contamination is often present in N_2 gas bottles. NO_x can be reduced to ammonia much more easily than N_2; consequently, since its presence could lead to a false positive, it is important to account for it. Nitrite, NO_2^-, can easily be detected down to 10 ppb with colorimetric tests. For the aqueous electrolyte, a known concentration of KNO_2 (≥ 96.0%, Sigma Aldrich) was added to 0.1 M KOH, then neutralized by adding 0.5 M H_2SO_4. Subsequently 35 mg of powder was added from a nitrite test kit (photometric 0.002-1.00 mg/l NO_2-N 0.007 - 3.28 mg/l NO_2^- Spectroquant®, Merck, Germany), containing sulfanilic acid and diazonium salt, to 3 ml of the neutralized solution. This was incubated for 10 min at room temperature before being analyzed by UV-vis spectrometry. A calibration curve was constructed with the same nitrite concentrations as the ammonia calibration; the fitted curve for the calibration showed a linear regression with an R-squared value of 0.99933.

Hydrazine can potentially be produced during ammonia synthesis. For the aqueous electrolyte, a known concentration of hydrazine monohydrate (~64%, Sigma Aldrich) was added to 0.1 M KOH, then neutralized by adding 0.5 M H_2SO_4. This was followed by adding 1 ml of the reagent solution from the hydrazine test kit (photometric 0.005 - 2.00 mg/l N_2H_4 Spectroquant®, Merck, Germany), containing 4-(dimethylamino)benzaldehyde, to 2.5 ml of the neutralized solution, and the new solution was incubated for 5 min at room temperature, before being analyzed by UV-vis spectrometry. A calibration curve was constructed with the same hydrazine concentrations as the ammonia calibration; the fitted curve for the calibration showed a linear regression with an R-squared value of 0.99999.

Single compartment cells. have the advantage of removing one parameter of possible ammonia contamination: the membrane. The single-compartment cell used in this work consisted of a clean glass cell containing 5 ml 0.1 M KOH electrolyte, with Ru as WE and Ir as CE, using a glass bubbler to saturate the electrolyte with N_2 gas. However, when we added 1 ppm of ammonia to such a setup in order to evaluate the efficiency of ammonia retrieval, using Ar gas (5.0, AGA Gas AB, Sweden) instead of N_2 (to exclude contamination from the gas stream), and applied potentials around -2.5 V vs. RHE for 1 hour, only 46 ppb and 54 ppb of the added ammonia could be recovered in two separate experiments. Ammonia was removed from the electrolyte, either by hydrogen bubble formation at the WE or by oxidation at the CE.

An acid or water trap downstream of the electrochemical cell. is often used to capture gas phase ammonia. However, due to the high solubility of ammonia in water, it tends to remain in aqueous electrolytes even at very high pH-values[33]. Therefore, one must evaluate the need for a downstream trap, as it is potentially redundant. Moreover, such a downstream trap could also be a serious source of contamination between experiments. We have not implemented a downstream trap.

Nafion. is a commonly used membrane and binder. In order to assess the influence of a Nafion membrane, we conducted a series of measurements in the two-compartment cell with 7.5 ml 0.1 M KOH as electrolyte, Ru as WE and Ir as CE, both with the "as-used" working electrolyte and after adding a set amount of ammonia. The Nafion (Nafion 117, Chemours) was either used as received, or pre-cleaned by boiling it for 1 hour in 3% H_2O_2 (30%, Merck, Germany), boiling it for 1 hour in 0.1 M H_2SO_4, and then rinsing in Millipore water to remove excess acid. We observed a reduction in the concentration of ammonia in 0.1 M KOH solutions in contact with fresh Nafion. This is due to the membrane soaking up background contamination of ammonia from the electrolyte it is submerged in, relative to a blank sample from the same batch of 0.1 M KOH, which had not been in contact

with Nafion. This leads to a "negative" concentration relative to the blank, as shown in Extended Data Figure 1A. On the other hand, when the Nafion is pre-cleaned using the aforementioned method, the membrane becomes a source of ammonia contamination. The membrane likely absorbs ammonia from the acid during cleaning, which is later released. Moreover, with no applied potential, the membrane allows for significant crossover of ammonia from the WE compartment to the CE compartment (1 ppm added to WE, recovered 945 ppb in WE and 178 ppb in CE after 1 hour). With applied potential the ammonia from the CE compartment becomes negative (1 ppm added to WE, recovered 925 ppb in WE and -20 ppb in CE after 1 hour at -0.5 V vs RHE with Ar), most likely due to a combination of oxidization at the CE and absorption into the membrane. Since Nafion can both be sink or source of ammonia, it should be used with great care in ammonia synthesis.

Celgard. The Celgard 3401 membrane is a 25 μm thick microporous polypropylene membrane. No significant increase or decrease in the detected levels of adventitious ammonia is measured with this membrane, shown in Extended Data Figure 1B. When 1 ppm of ammonia is added to the working electrode compartment at OCP, all of the ammonia was recovered. With an applied potential of -2.5 V vs RHE using Ar gas, crossover across the membrane increases, and 791 ppb of the 1 ppm of ammonia added was recovered from the WE compartment, and 89 ppb was recovered at the CE compartment. An H-cell with the Celgard membrane was therefore used for all aqueous experiments.

Additional sources of contamination. Three clean glass vials separately containing 2 ml 0.1 M KOH, 2 ml Millipore H_2O, and 2 ml 0.1 M $HClO_4$ were left open in the laboratory. After 24 hours, they contained significant amounts of ammonia, as shown in Extended Data Figure 1C, repeated three times on different days. To show the possible contamination from human breath, an experiment in which one participant exhaled 3 L (close to the average human full-breath capacity) through a glass tube inserted into 2 ml of 0.1 M KOH was conducted and repeated in 3 measurements. Extended Data Figure 1D shows that the amount of ammonia accumulated in this manner can be significant. Additionally, nitrile rubber gloves are commonly used in laboratory work. Nitrile rubber is a copolymer of acrylonitrile and butadiene. Acrylonitrile is typically produced by catalytic ammoxidation of propylene, where ammonia is used as a reactant. We sonicated a ~ 5 cm^2 of a nitrile glove (Pharma und Kosmetik GmbH, Germany) in 10 ml DI-water for 1 h, and 2.8 ppm was detected by the indophenol method. Care must therefore be taken when using nitrile gloves in ammonia synthesis.

We stress that the contamination levels that we observed herein are not definitive: they depend on cleaning procedures and environmental factors like ambient ammonia concentration. Nonetheless our experiments provide examples of how contamination in a given set-up can be quantified.

Mass spectrometry (MS). Isotope labelled ammonia can be detected via MS ue to the atomic weight difference between $^{14}NH_3$ and $^{15}NH_3$. Unfortunately, H_2O has a mass difference of only 0.008 amu compared isotope labelled $^{15}NH_3$, so suppression of the water signal, e.g. by lowering the ionization potential coupled with very high resolution, could quantify the $^{15}NH_3$ signal. Other strategies to mitigate the interference from water have thus far only yielded qualitative data[21].

Gas phase FTIR spectroscopy. FTIR can distinguish between $^{14}NH_3$ and $^{15}NH_3$, based on the atomic mass difference and the corresponding change to the vibrational frequencies. This manifests itself as a roughly 5 wavenumber shift in the wagging mode of ammonia (see Extended Data Figure 3) centered around 940 wavenumbers, in accordance with the prediction of the quantum mechanical harmonic oscillator[22].

Nuclear magnetic resonance (NMR) spectroscopy. All NMR experiments were performed at 25 °C on a Bruker AVANCEIII HD spectrometer operating at a ^1H frequency of 800.182 MHz and equipped with a 5mm TCI CryoProbe (Bruker Biospin) or a Bruker AVANCE III HD spectrometer operating at a ^1H frequency of 400.13 MHz equipped with a Prodigy probe (Bruker Biospin). One way to confirm the successful electrochemical production of NH_3 from isotope labelled $^{15}N_2$ experiments could be a standard "pulse and acquire" NMR experiment tuned to the resonance frequency of ^{15}N. Despite using a ^{15}N-labeled precursor, the low production yield, coupled with unfavorable NMR properties of ^{15}N (e.g. low gyromagnetic ratio and long T1 relaxation constants) limits the sensitivity of ^{15}N for this application. ^1H NMR is the better choice for sensitivity, as it can differentiate $^{15}NH_4^+$ from $^{14}NH_4^+$, since ^{14}N is a spin-1 nucleus and ^{15}N is a spin-½ nucleus. Consequently, the scalar interaction between ^1H and ^{15}N in $^{15}NH_4^+$ results in a splitting of the ^1H resonance into two symmetric signals, with a spacing of 73 Hz; the magnitude of the ^1H-^{15}N scalar interaction. On the other hand, the ^1H resonance for ^1H coupled to ^{14}N in $^{14}NH_4^+$ is split into three symmetric signals with a spacing of 52 Hz. For the samples prepared in H_2O the water resonance was suppressed with the excitation sculpting method using a 3 ms 180° shaped pulse centered at 4.70 ppm. The perfect-echo variant was chosen to reduce J- modulation for the samples analyzed at 800 MHz. A total of 1024 transient scans were recorded with an inter-scan delay of 1 second. 64K complex points was acquired for each FID with an acquisition time of 3.4 seconds. The processed spectra have been zero-filled to 64K real points and an exponential apodization function with lb = 0.3 Hz was applied prior to Fourier transformation (FT). 3 vol.% D_2O (99.9%, Sigma Aldrich, Denmark) was added for deuterium locking and referencing. For the samples analyzed at 400 MHz it was necessary to add 10 vol.% D_2O for sufficient lock signal. For the samples prepared in THF/ethanol the 1D-NOESY pre-saturation method was utilized to suppress the two THF signals. A train of 100 ms square pulses centered at 3.66 ppm with a frequency modulation of 1.82 ppm was applied during the relaxation delay (3 seconds) and mixing time (100 ms). ^{13}C cw-decoupling was applied during the acquisition time to decrease the intensity of the THF satellite signals. A total of 512 transient scans were recorded. 16K complex points was acquired for each FID with an acquisition time of 3.4 seconds. Linear prediction was used to double the number of complex points and the FID was subsequently zero-filled to 32K real points. An exponential apodization function with lb = 1Hz was applied prior to FT. 5 vol.% THF-d8 (99.9%, Sigma Aldrich, Denmark) was added for deuterium locking and referencing. Calibration samples were prepared with varying concentrations of $^{14}NH_4Cl$ (99.8%, Merck, Germany) and $^{15}NH_4Cl$ (98 atom% ^{15}N, Sigma Aldrich, Denmark).

Gas circulation setup for isotope measurements. While we stress the importance of isotope labelling experiments, we acknowledge the high price and small volume of $^{15}N_2$ gas bottles makes such measurements challenging. Furthermore, the low activity of the nitrogen reduction reaction requires the experiment to run for an extended time, with a continuous supply of N_2 gas. Typically, a few litres or tens of litres are required for each measurement, and most of the gas is lost as exhaust. Nevertheless, the price of USD 2,100 for 5 liters 98% $^{15}N_2$ is nothing compared to having an incorrect scientific report published, which potentially can mislead the entire field. Therefore, we designed a circulation setup where $^{15}N_2$ gas was continuously cycled and re-supplied to the electrode surface. A simplified schematic and picture of our setup is shown in Extended Data Figure 4. A 4-way valve is central to the set-up, and enables the choice between purging mode, i.e. gas flowing through the entire set-up to the exhaust, and circulating mode, i.e. gas being cycled in the enclosed system by a pump. The volume of the enclosed cycling system is about 100 ml (4.46 mmol N_2), which for the present conversion range is plenty. The inlet gas passes through a Cu impurity trap and a cold trap, described in detail in the following section, to remove any impurity supplied to the system. A water trap before the exhaust limits the possibility of back flow. Before flowing $^{15}N_2$ gas, Ar gas is first flowed through the whole set-up for 30 min to remove any $^{14}N_2$ gas that was present in the system. After sufficient purging with Ar, $^{15}N_2$ is flowed for 20 min with a flow rate of 10 ml min^{-1}. Then the 4-way valve is switched to circulating mode, and the isotope experiments were performed. $^{14}N_2$ experiments were performed in the exactly the same manner, except for the unnecessary Ar purging beforehand. The setup also allows the flow of 10% H_2 in Ar through the gas line that is used for the activation of the copper catalyst.

Cleaning of $^{15}N_2$ gas. Cleaning of the $^{15}N_2$ gas (98 atom% ^{15}N, Sigma Aldrich) is very important, since $^{15}N_2$ may contain significant impurities, in the form of $^{15}NH_3$ along with $^{15}NO_x$ species[10]. We tested the purity of our $^{15}N_2$ by first saturating our solution of 0.1 M KOH with Ar to remove any excess $^{14}N_2$, followed by bubbling ~ 200 ml of $^{15}N_2$. We circulated the 200 ml $^{15}N_2$ gas for 1 h to duplicate the long-term electrochemical measurement. The resulting solution was analyzed via colorimetric tests to detect NH_3, NO_2^-, and N_2H_4 and NMR to differentiate $^{14}NH_4^+$ from $^{15}NH_4^+$. With NMR spectroscopy, shown in Extended Data Figure 5, we observed a detectable amount of $^{14}NH_4^+$, which is as an unavoidable impurity. However, we could not observe any $^{15}NH_4^+$ species. Colorimetric tests also confirmed <10 ppb of NH_3 in the solution, seen in Extended Data Figure 6A. Given the result, we concluded that $^{15}NH_3$ contamination for our system is negligible. Unlike ammonia, we clearly observed >10 ppb of nitrite from the colorimetric test, as seen Extended Data Figure 6C. NO_2^- can easily be reduced to NH_4^+ and would give a false positive, even in the isotope labelled tests. To remove these impurities, a Cu impurity trap was introduced, composed of 2 g Cu-Zn-Al oxide catalyst in a U shaped stainless steel tubing[34,35]. The Cu catalyst was reduced before each experiment in a 5% H_2/Ar stream at 300 °C for 2 hours. The gas flow was switched to Ar at 300 °C for 30 min, and the Cu impurity trap was cooled down to –100 °C using an ethanol slurry, prepared by mixing ethanol with liquid nitrogen. Ar flow through the Cu impurity trap was used to purge out the entire system for 30 min, including the gas tight electrochemical cell. The electrolyte was then injected using a syringe to the Ar purged electrochemical cell to prevent exposure to air and moisture. Ar was bubbled through the electrolyte for an additional 30 min to remove dissolved $^{14}N_2$. Finally, $^{15}N_2$ was introduced to the electrochemical system through the reduced Cu impurity trap. After bubbling $^{15}N_2$ gas for 15 min (~200 ml), the gas was circulated in a closed loop using a glass pump (Makuhari Rikagaku Garasu Inc., Japan). Using this cleaning procedure, three repeated measurements were carried out. The first test with the cleaning procedure showed up to 25 ppb of ammonia, as seen in Extended Data Figure 6B. We assume this to be due to leftover contamination of the catalyst, or unaccounted impurity from the environment. Both, however, were in the form of $^{14}NH_4^+$ as seen with NMR, and should therefore not interfere with

the isotope labelling measurements. For the 2nd and 3rd tests with the cleaning procedure, no ammonia was detected. For nitrite measurements, small amounts of nitrite in the gas stream was clearly removed, and we could not detect any nitrite after the cleaning procedure, as seen in Extended Data Figure 6D. No hydrazine was measured before the cleaning procedure as seen in Extended Data Figure E. Such a cleaning procedure is important to definitively prove the catalytic conversion from $^{15}N_2$ to $^{15}NH_3$. Other techniques may be utilized to clean the $^{15}N_2$ gas, such as using a commercial gas purifier (MicroTorr MC1-902F, SAES Pure Gas), with certified $<$ 5 pptV of NH_3 and $<$ 1 pptV of NO_X impurities.

Data availability

The datasets generated during and/or analysed during the current study are available from the corresponding author on reasonable request.

31. Čolić, V. *et al*. Experimental Aspects in Benchmarking of the Electrocatalytic Activity. *ChemElectroChem* **2**, 143–149 (2015).
32. Gritzner, G. Standard electrode potentials of $M^+|M$ couples in non-aqueous solvents (molecular liquids). *J. Mol. Liq.* **156**, 103–108 (2010).
33. Brass, M., Pritzel, T., Schulte, E., and Keller, J. U. Measurements of Vapor-Liquid Equilibria in the Systems NH_3-H_2O-NaOH and NH_3-H_2O-KOH at Temperatures of 303 and 318 K and Pressures 0.1 MPa$<$p$<$1.3 MPa. *Int. J. Thermophys.* **21**, 883–898 (200AD).
34. Ma, L. *et al*. In situ DRIFTS and temperature-programmed technology study on NH_3-SCR of NO_x over Cu-SSZ-13 and Cu-SAPO-34 *catalysts. Appl. Catal. B Environ*. **156–157**, 428–437 (2014).
35. Ma, L. *et al*. Characterization of commercial Cu-SSZ-13 and Cu-SAPO-34 catalysts with hydrothermal treatment for NH_3-SCR of NO_x in diesel exhaust. *Chem. Eng. J.* **225**, 323–330 (2013).
36. Cook, R. L. & Sammells, A. F. Ambient temperature gas phase electrochemical nitrogen reduction to ammonia at ruthenium/solid polymer electrolyte interface. *Catal. Letters* **1**, 345–349 (1988).
37. Furuya, N. & Yoshiba, H. Electroreduction of nitrogen to ammonia on gas-diffusion electrodes modified by Fe-phthalocyanine. *J. Electroanal. Chem. Interfacial Electrochem.* **263**, 171–174 (1989).
38. Furuya, N. & Matsui, K. Electroreduction of carbon dioxide on gas-diffusion electrodes modified by metal phthalocyanines. *J. Electroanal. Chem. Interfacial Electrochem.* **271**, 181–191 (1989).
39. Kordali, V., Kyriacou, G. & Lambrou, C. Electrochemical synthesis of ammonia at atmospheric pressure and low temperature in a solid polymer electrolyte cell. *Chem. Commun*. 1673–1674 (2000). https://doi.org/10.1039/b004885m
40. Pospíšil, L. *et al*. Electrochemical conversion of dinitrogen to ammonia mediated by a complex of fullerene C_{60} and γ-cyclodextrin. *Chem. Commun*. 2270–2272 (2007). https://doi.org/10.1039/B701017F
41. Xu, G., Liu, R. & Wang, J. Electrochemical synthesis of ammonia using a cell with a Nafion membrane and $SmFe_{0.7}Cu_{0.3-x}Ni_xO_3$ (x = 0–0.3) cathode at atmospheric pressure and lower temperature. *Sci. China Ser. B Chem.* **52**, 1171–1175 (2009).
42. Kugler, K., Luhn, M., Schramm, J. A., Rahimi, K. & Wessling, M. Galvanic deposition of Rh and Ru on randomly structured Ti felts for the electrochemical NH_3 synthesis. *Phys. Chem. Chem. Phys.* **17**, 3768–3782 (2015).
43. Li, S.-J. *et al*. Amorphizing of Au Nanoparticles by CeO_x -RGO Hybrid Support towards Highly Efficient Electrocatalyst for N_2 Reduction under Ambient Conditions. *Adv. Mater.* **29**, 1700001 (2017).
44. Chen, S. *et al*. Electrocatalytic Synthesis of Ammonia at Room Temperature and Atmospheric Pressure from Water and Nitrogen on a Carbon-Nanotube-Based Electrocatalyst. *Angew. Chemie Int. Ed.* **56**, 2699–2703 (2017).
45. Marnellos, G. Ammonia Synthesis at Atmospheric Pressure. *Science (80-.).* **282**, 98–100 (1998).
46. Murakami, T., Nohira, T., Goto, T., Ogata, Y. H. & Ito, Y. Electrolytic ammonia synthesis from water and nitrogen gas in molten salt under atmospheric pressure. *Electrochim. Acta* **50**, 5423–5426 (2005).
47. Wang, B. H., Wang, J. De, Liu, R., Xie, Y. H. & Li, Z. J. Synthesis of ammonia from natural gas at atmospheric pressure with doped ceria–$Ca_3(PO_4)_2$–K_3PO_4 composite electrolyte and its proton conductivity at intermediate temperature. *J. Solid State Electrochem.* **11**, 27–31 (2006).
48. Köleli, F. & Kayan, D. B. Low overpotential reduction of dinitrogen to ammonia in aqueous media. *J. Electroanal. Chem.* **638**, 119–122 (2010).
49. Amar, I. A. *et al*. Electrochemical synthesis of ammonia based on doped-ceria-carbonate composite electrolyte and perovskite cathode. *Solid State Ionics* **201**, 94–100 (2011).
50. Amar, I. A., Lan, R., Petit, C. T. G., Arrighi, V. & Tao, S. Electrochemical synthesis of ammonia based on a carbonate-oxide composite electrolyte. *Solid State Ionics* **182**, 133–138 (2011).
51. Amar, I. A. *et al*. Electrochemical synthesis of ammonia from N_2 and H_2O based on $(Li,Na,K)_2CO_3$–$Ce_{0.8}Gd_{0.18}Ca_{0.02}O_{2-\delta}$ composite electrolyte and $CoFe_2O_4$ cathode. *Int. J. Hydrogen Energy* **39**, 4322–4330 (2014).
52. Licht, S. *et al*. Ammonia synthesis by N_2 and steam electrolysis in molten hydroxide suspensions of nanoscale Fe_2O_3. *Science (80-.).* **345**, 637–640 (2014).
53. Lan, R., Alkhazmi, K. A., Amar, I. A. & Tao, S. Synthesis of ammonia directly from wet air at intermediate temperature. *Appl. Catal. B Environ.* **152–153**, 212–217 (2014).
54. Amar, I. A., Lan, R. & Tao, S. Electrochemical Synthesis of Ammonia Directly from Wet N_2 Using $La_{0.6}Sr_{0.4}Fe_{0.8}Cu_{0.2}O_{3-\delta}$-$Ce_{0.8}Gd_{0.18}Ca_{0.02}O_{2-\delta}$ Composite Catalyst. *J. Electrochem. Soc.* **161**, H350–H354 (2014).
55. Amar, I. A., Lan, R., Petit, C. T. G. & Tao, S. Electrochemical Synthesis of Ammonia Based on Co_3Mo_3N Catalyst and $LiAlO_2$–$(Li,Na,K)_2CO_3$ Composite Electrolyte. *Electrocatalysis* **6**, 286–294 (2015).
56. Cui, B. *et al*. Electrochemical synthesis of ammonia directly from N_2 and water over iron-based catalysts supported on activated carbon. *Green Chem.* **19**, 298–304 (2017).
57. Van Tamelen, E. E. & Akermark, B. Electrolytic reduction of molecular nitrogen. *J. Am. Chem. Soc.* **90**, 4492–4493 (1968).
58. Becker, J. Y., Avraham (Tsarfaty), S. & Posin, B. Nitrogen fixation: Electrochemical reduction of titanium compounds in the presence of catechol and N_2 in MeOH or THF. *J. Electroanal. Chem. Interfacial Electrochem.* **230**, 143–153 (1987).
59. Köleli, F. & Röpke, T. Electrochemical hydrogenation of dinitrogen to ammonia on a polyaniline electrode. *Appl. Catal. B Environ.* **62**, 306–310 (2006).
60. Kim, K. *et al*. Communication—Electrochemical Reduction of Nitrogen to Ammonia in 2-Propanol under Ambient Temperature and Pressure. *J. Electrochem. Soc.* **163**, F610–F612 (2016).
61. Zhu, D., Zhang, L., Ruther, R. E. & Hamers, R. J. Photo-illuminated diamond as a solid-state source of solvated electrons in water for nitrogen reduction. *Nat. Mater.* **12**, 836–841 (2013).
62. Dong, G., Ho, W. & Wang, C. Selective photocatalytic N_2 fixation dependent on g-C_3N_4 induced by nitrogen vacancies. *J. Mater. Chem. A* **3**, 23435–23441 (2015).
63. Banerjee, A. *et al*. Photochemical Nitrogen Conversion to Ammonia in Ambient Conditions with FeMoS-Chalcogels. *J. Am. Chem. Soc.* **137**, 2030–2034 (2015).
64. Li, J., Li, H., Zhan, G. & Zhang, L. Solar Water Splitting and Nitrogen Fixation with Layered Bismuth Oxyhalides. *Acc. Chem. Res.* **50**, 112–121 (2017).
65. Liu, J. *et al*. Nitrogenase-mimic iron-containing chalcogels for photochemical reduction of dinitrogen to ammonia. *Proc. Natl. Acad. Sci.* **113**, 5530–5535 (2016).
66. Hu, S. *et al*. Effect of Cu(I)–N Active Sites on the N_2 Photofixation Ability over Flowerlike Copper-Doped g-C_3N_4 Prepared via a Novel Molten Salt-Assisted Microwave Process: The Experimental and Density Functional Theory Simulation Analysis. *ACS Sustain. Chem. Eng.* **5**, 6863–6872 (2017).
67. Hirakawa, H., Hashimoto, M., Shiraishi, Y. & Hirai, T. Photocatalytic Conversion of Nitrogen to Ammonia with Water on Surface Oxygen Vacancies of Titanium Dioxide. *J. Am. Chem. Soc.* **139**, 10929–10936 (2017).

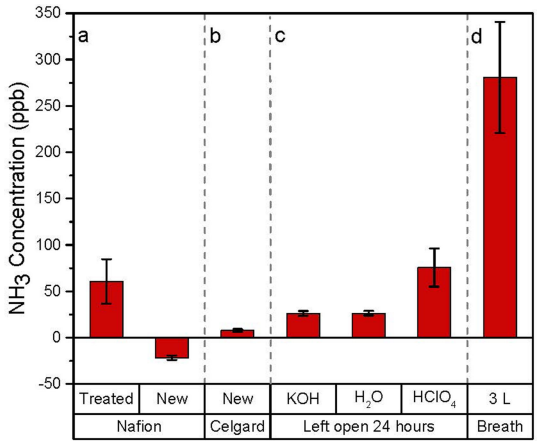

Extended Data Fig. 1 | Concentrations of ammonia produced by various possible contamination sources. All measurements are repeated 3 times, displaying the mean and standard deviation. a) New and treated Nafion membranes, b) New Celgard membrane, c) Leaving 2 ml of 0.1 M solutions or MilliQ H_2O open overnight, d) One person breathing 3L air through a glass straw into 2 ml 0.1 M KOH.

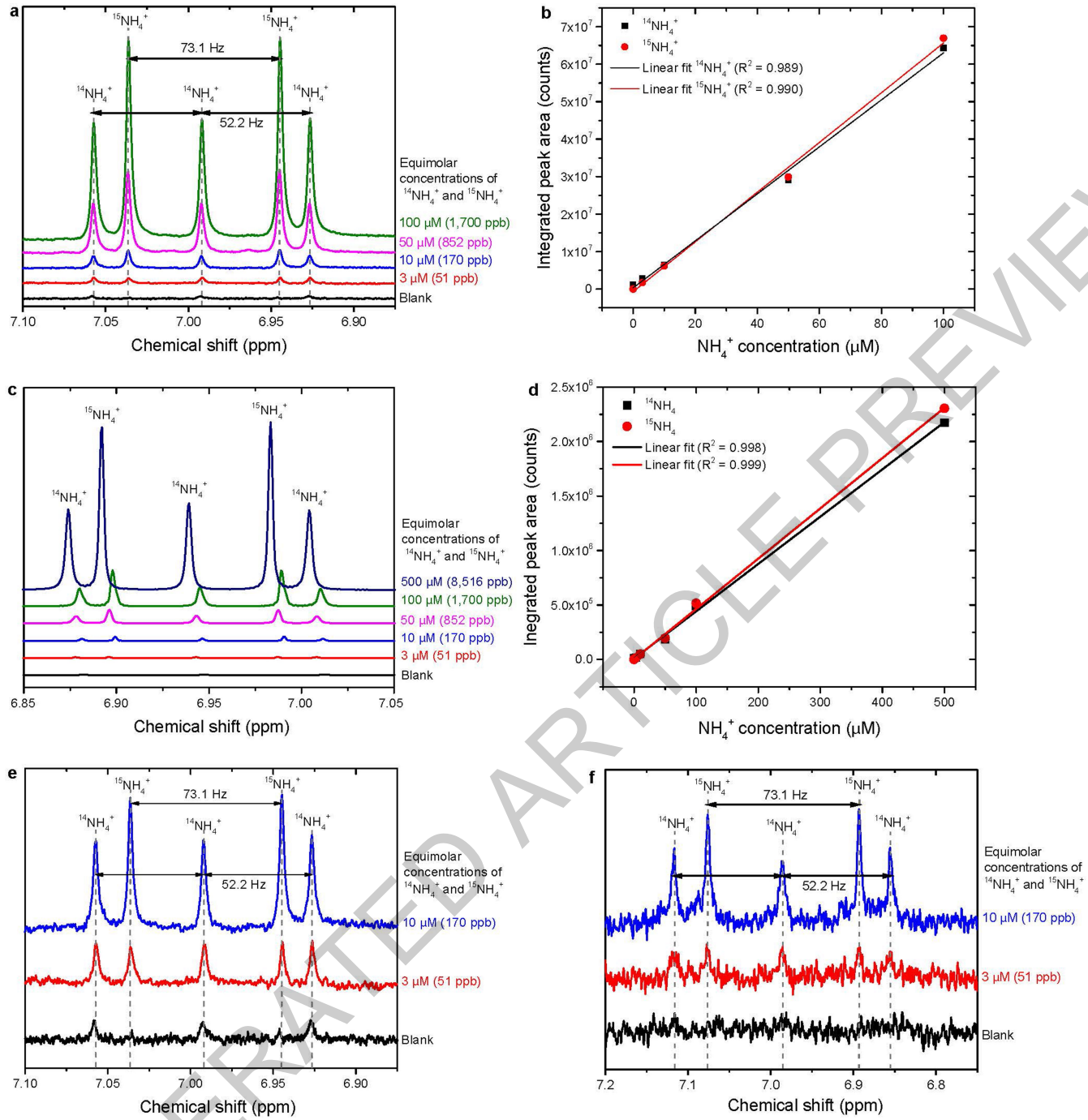

Extended Data Fig. 2 | NMR data acquired with a Bruker Avance III HD 800 MHz spectrometer equipped with a 5 mm TCI CryoProbe. Solutions contain equal concentrations of $^{14}NH_4^+$ and $^{15}NH_4^+$ from NH_4Cl. a Solution of 600 µl 0.1M KOH, acidified with 0.5 M H_2SO_4 to a pH of 1. 200 µM CH_3OH added as internal reference. **b** Integrated peak area from **a** for both $^{14}NH_4$ and $^{15}NH_4$. **c** Solution of 500 µl 0.1 M $LiClO_4$ in THF and ethanol with a ratio of 99:1, respectively with 2 µl 4M HCl and 50 µl d-THF. **d** Integrated peak area from **c** for both $^{14}NH_4$ and $^{15}NH_4$. Variation of chemical shift of NMR peaks is due to slight differences in pH, volume, and/or temperature of samples. **e** Zoom of lower concentrations from **a**. **f** Same concentrations and solution as **a**, using Bruker AVANCE III HD 400 MHz spectrometer equipped with a 5 mm Prodigy probe.

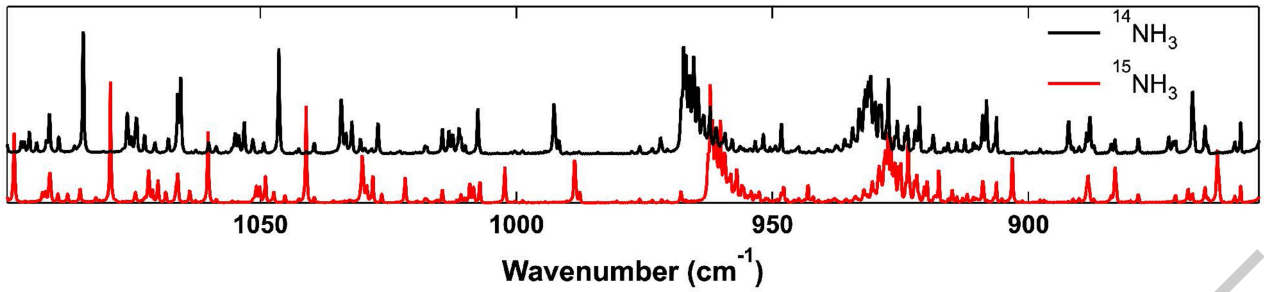

Extended Data Fig. 3 | Gas phase FTIR spectra of labelled and unlabeled ammonia acquired on a Nicolet iS50 spectrometer fitted with a 2m path length gas cell heated to 135°C. Total volume of vaporized sample is 100 µl. Ammonia concentration was 1000 ppm in H_2O prior to vaporization.

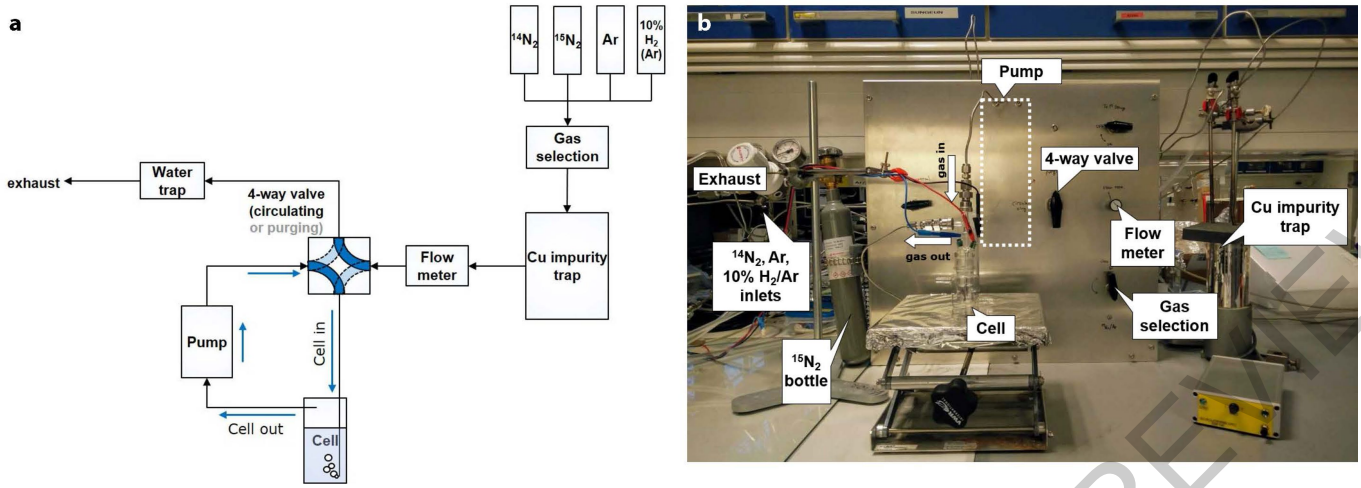

Extended Data Fig. 4 | The setup for gas ($^{15}N_2$, $^{14}N_2$, Ar, or 10% H_2 in Ar) circulation through the electrochemical cell (A) schematics of the setup (B) photograph of the setup with the components denoted. The pump that circulates the gas through the setup is situated behind the metal panel, and its position is outlined by the white dashed rectangle.

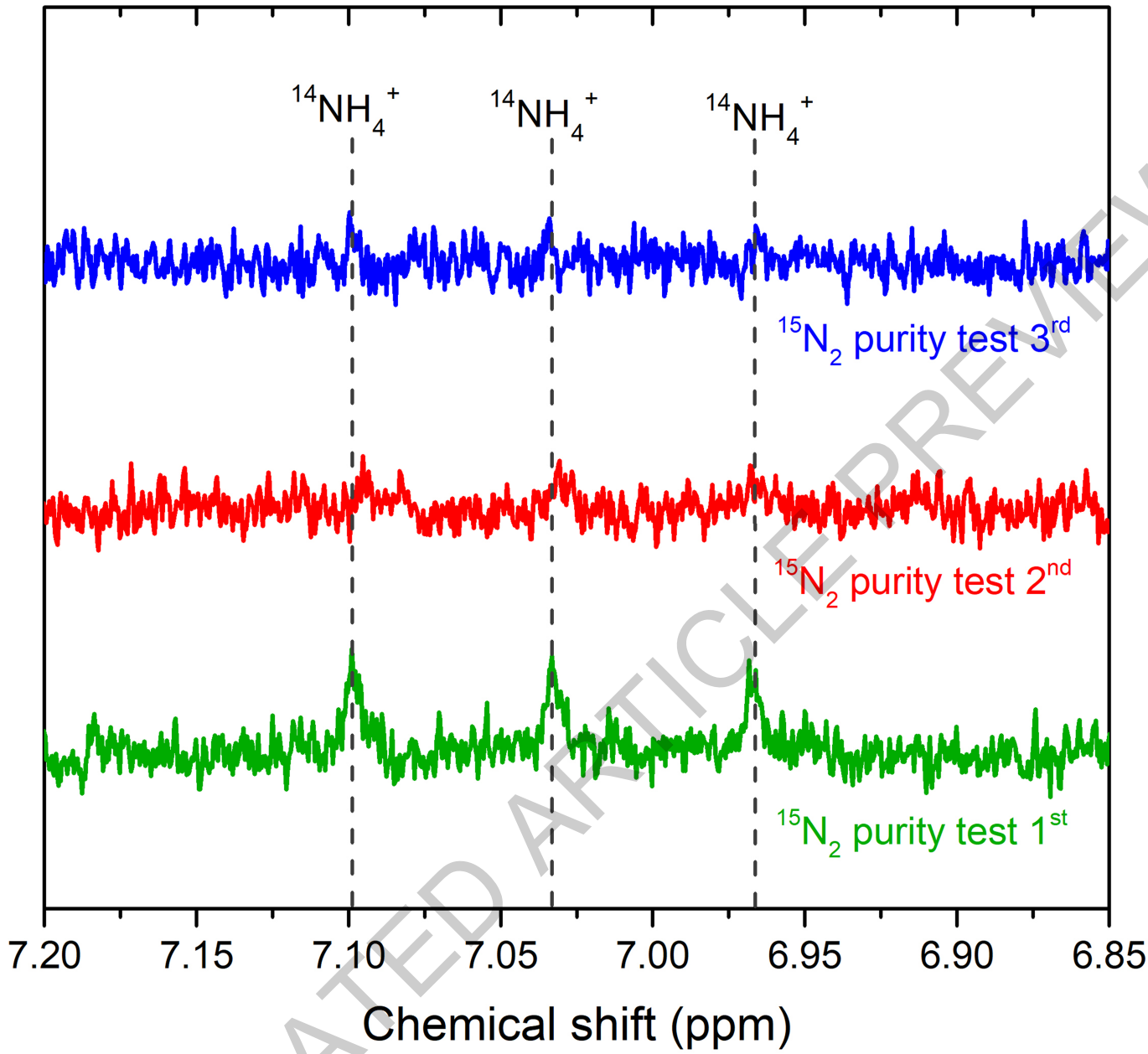

Extended Data Fig. 5 | The 1H NMR spectra of the samples after purging the solution with $^{15}N_2$ gas using Bruker AVANCE III HD 800 MHz spectrometer equipped with a 5 mm TCI CryoProbe. No $^{15}NH_4^+$ was seen in the measurements.

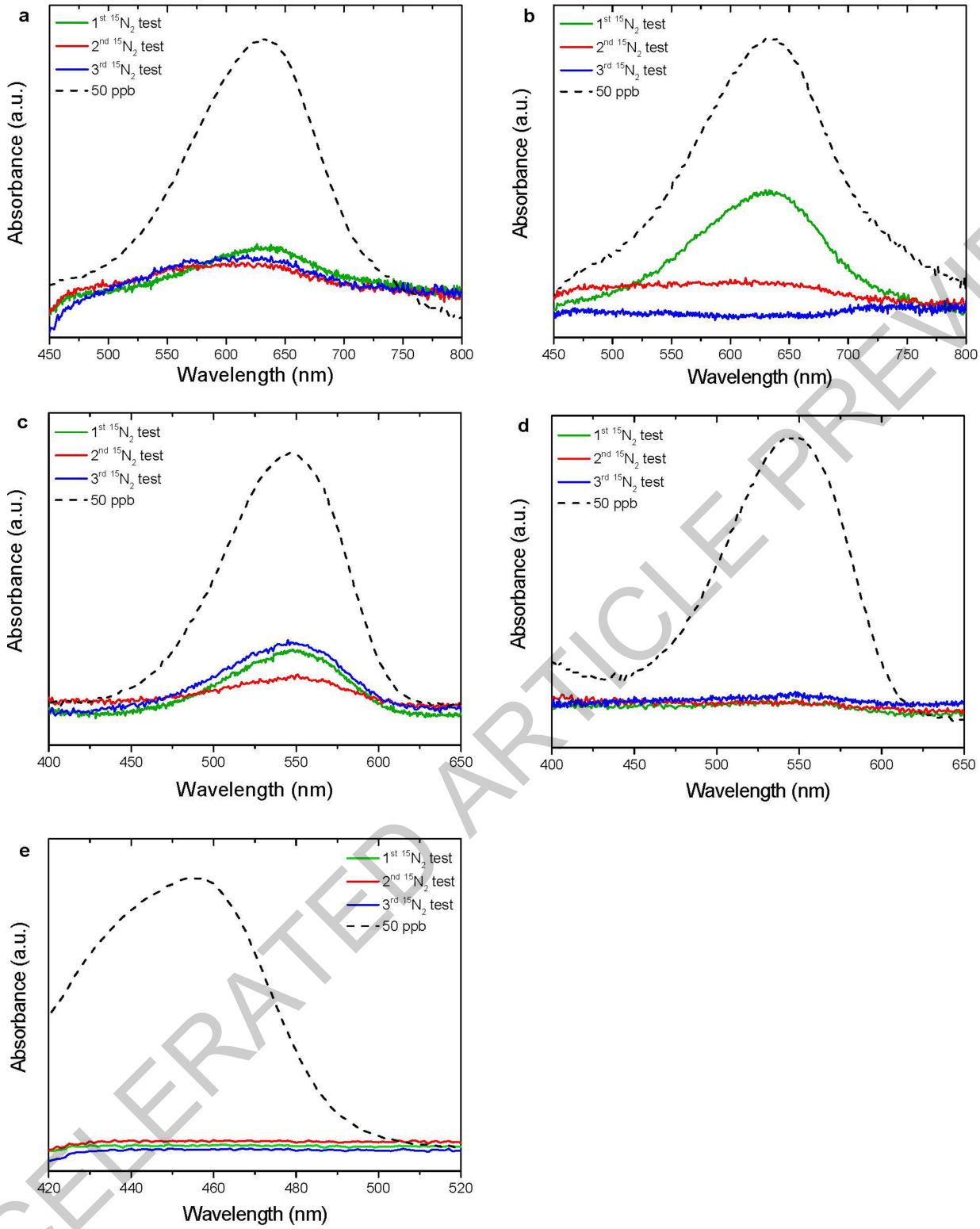

Extended Data Fig. 6 | Concentration measurements of ammonia, nitrite, and hydrazine in the gas supply. Three sequentially repeated concentration measurements of: **a** ammonia via indophenol without cleaning the gas stream, **b** ammonia via indophenol with the applied cleaning procedure, **c** nitrite concentration without cleaning the gas stream, **d** nitrite concentration with the applied cleaning procedure, and **e** hydrazine concentration without cleaning the gas stream.

Extended Data Table 1 | Literature data on electrochemical N2 reduction to ammonia in near-ambient condition

Reference	Catalyst	Reactant	Electrolyte	T (°C)	E(V)	Rate (μmol h^{-1} cm^{-2})	FE (%)	C_{NH3} (ppm)	Comment	^{15}N
Sclafani et al. (1983)[7]	Fe	N_2, H_2O	6 N KOH	45	-1.06 V vs SCE	0.0002	-	-	Polyethylene membrane No specified blank test Acid trap used	no
Cook et al. (1988)[36]	Ru	N_2, H_2	Nafion	25	-	1.75×10^{-3}	0.0015	-	Ar blank test Open-ciruit blank test Acid trap used	no
Furuya et al. (1989)[37]	Fe-phthalocyanine	N_2, H_2	1 M KOH	25	-	2.02 ~ 0.680	0.34 ~0.12	-	No blank test	no
Furuya et al. (1989)[38]	Sn-phthalocyaine	N_2, H_2	1 M KOH	25	-0.4 V vs RHE	-	1.83 ~1.18	-	No blank test	no
Furuya et al. (1990)[37]	Fe PbO-TiO_2 ZnS ZnSe	N_2, H_2	1 M KOH	25	-1.0 V vs RHE	4.82 3.37 20.4 23.2	0.12 0.27 0.96 1.29	-	No blank test	no
Kordali et al. (2000)[39]	Ru	N_2, H_2O	Nafion	90	-1.02 V vs Ag/AgCl	0.076	0.24	4.89 * (acid trap)	Nafion used Open curcuit blank test Ar blank test	no
Pospíšil et al. (2007)[40]	C_{60}-γ-cyclodextrin complex / Hg electrode	N_2, H_2O	0.1 M KCl	60	-1.2 V vs Ag/AgCl	-	-	-	No blank test Acid trap used	no
Xu et al. (2009)[41]	$SmFe_{0.7}Cu_{0.1}Ni_{0.2}O_3$	N_2, H_2	Nafion	80	2.0 V (two-electrodes)	40.7	90.4	19.6 * (acid trap)	Nitrates used in synthesis NH_3 used in synthesis Acid trap used No blank test	no
Zhang et al. (2010)[8]	$SmBaCuNiO_{5+\delta}$	N_2, H_2	Nafion	80	2.5 V (two-electrodes)	31.3	-	15.1 * (acid trap)	Nitrates used in synthesis Ammonia used in synthesis Acid trap used No blank test	no
Lan et al. (2013)[9]	Pt	Air, H_2O	NH_4^+ exchanged Nafion	80	1.6 V (two-electrodes)	4.10	0.51	-	NH_4^+ exchanged Nafion Acid trap used No blank test	no
Kugler et al. (2015)[42]	Ru	N_2, H_2	0.5 M H_2SO_4	25	-	0.432	-	0.58	$(NH_4)_3[\{RuCl_4(H_2O)\}_2(\mu\text{-}N)]$ used for preparing Ru electrode Acid electrolyte No blank test	no
Bao et al. (2017)[25]	Tetrahexahedral Au nanoparticles	N_2, H_2O	Nafion, 0.1 M KOH	25	-0.2 V vs RHE	0.0968	4.00	41.2 * ppb/hr	Nitrate used in synthesis Cetyltrimethylammonium bromide used in synthesis Ar blank test Open circuit blank test	no
Li et al. (2017)[43]	Amorphous Au nanoparticles/CeO_X-RGO	N_2, H_2O	0.1 M HCl, Nafion	25	-0.2 V vs RHE	-	10.10	-	Nitrate used in synthesis Ar blank test Open circuit blank test	no
Shi et al. (2017)[18]	Au sub-nano clusters on TiO_2	N_2, H_2O	0.1M HCl, Nafion	25	-0.2 V vs RHE	-	8.11	-	Ar blank test Open circuit blank test	no
Chen et al. (2017)[44]	Fe_2O_3/carbon nanotubes	N_2, H_2O	Nafion	20	-2.0 V vs Ag/AgCl	0.013	0.027	-	Open circuit blank test	no
Chen at al. (2017)[26]	Li^+-incorporated poly(N-ethyl-benzene-1,2,4,5-tetracarboxylic diimide) (PEBCD)	N_2, H_2O	H_2SO_4 added 0.5 M Li_2SO_4, Nafion	25	-0.7 V vs RHE	0.11869	1.71	-	Diamine used in synthesis N as imide in catalyst, HNO_3 used in electrode preparation Ar blank test No catalyst blank test $^{15}N\equiv{}^{14}N$ gas used with NMR	yes
Kong et al. (2017)[27]	γ-Fe_2O_3 nanoparticles	N_2, H_2O	i) 0.1 M KOH ii) Anion-exchange membrane (FAA-3, Fumatech)	i) 25 ii) 65	i) 0.0 V vs RHE ii) 1.6 V (two-electrodes)	i) 0.044 ii) 0.056	i) 1.96 ii) 0.04	i) – ii) 0.252	Nafion used for half-cell Acid trap used for MEA Ar blank test	no
Yao et al. (2018)[28]	Au	N_2, H_2O	0.1 M KOH	25	-0.5 V vs RHE	0.014	0.12	0.14	Blank measurement performed for SEIRAS experiment, but not for catalytic test	no
Song et al. (2018)[21]	CNS (N- doped carbon nanospikes)	N_2, H_2O	0.25 M $LiClO_4$	25	-1.19 V vs RHE	5.71 ± 0.42	11.56 ± 0.85	69.97 * ± 5.13 *	Argon blank test Isotope labelled GCMS Blank tests without active catalyst	yes

Ambient conditions were noted as 25 °C.
All pressures were ambient. No reported TOF.
* denotes calculated (or estimated) concentrations from parameters given in the papers.

Extended Data Table 2 | Electrochemical N_2 reduction to ammonia at high temperature or pressure

Reference	Catalyst	Reactant	Electrolyte	T (°C)	P (atm)	E(V)	Rate (μmol h^{-1} cm^{-2})	FE (%)	C_{NH3} (ppm)	Comment	^{15}N
Marnellos et al. (1998)[45]	Pd	N_2, H_2	$SrCe_{0.95}Yb_{0.05}O_3$	570	1	-	17.4	78	-	OCV blank test Acid trap used	no
Murakami et al. (2005)[46]	Ni	N_2, H_2O	0.5 mol% Li_3N in molten LiCl–KCl–CsCl	300	1	0.4 V vs Li^+/Li	72	23	-	Not continuous process $N_2 \rightarrow Li_3N \rightarrow NH_3$	no
Wang et al. (2006)[47]	Ag-Pd	N_2, CH_4	Y doped Ce-$Ca_3(PO_4)_2$–K_3PO_4	650	1	1.0 V (two-electrodes)	25.0	-	-	Ammonium and nitrate salts used in synthesis Acid trap used No blank test	no
Köleli et al. (2010)[48]	Polypyrrole $(C_4H_2NH)_n$	N_2, H_2O	Aqueous 0.1 M Li_2SO_4/ 0.03 M H^+	25	59.2	- 0.165 V vs NHE	-	-	0.903 *	Ar blank test No catalyst blank test	no
Amar et al. (2011)[49]	$La_{0.6}Sr_{0.4}Fe_{0.8}Cu_{0.2}O_{3-\delta}$-$Ce_{0.8}Sm_{0.2}O_{2-\delta}$	N_2, H_2	$La_{0.6}Sr_{0.4}Fe_{0.8}Cu_{0.2}O_{3-\delta}$ and $Ce_{0.8}Sm_{0.2}O_{2-\delta}$	450	1	0.8 V (two-electrodes)	19.4	-	5.22 * (acid trap)	Nitrates used in synthesis Ammonia used in synthesis Acid trap used No blank test	no
Amar et al. (2011)[50]	$CoFe_2O_4$ with Ag	N_2, H_2	Carbonate-$LiAlO_2$ composite	400	1	0.8 V (two-electrodes)	0.835	-	0.512 * (acid trap)	Nitrate used in synthesis Ammonia used in synthesis Acid trap used No blank test	no
Amar et al. (2014)[51]	$CoFe_2O_4$-$Ce_{0.8}Gd_{0.18}Ca_{0.02}O_{2-\delta}$	N_2, H_2O	Ca,Gd co-doped Ce-ternary carbonate composite	400	1	1.6 V (two-electrodes)	0.234	0.17	0.156 * (acid trap)	Nitrate used in synthesis Ammonia used in synthesis Acid trap used No blank test	no
Licht et al. (2014)[52]	Fe_2O_3 (Ni-monel electrode)	N_2, H_2O	Molten NaOH/KOH	200	1	1.23 V (two-electrodes)	8.64	35	-	Ar blank test Open circuit blank test Water trap used	no
Lan et al. (2014)[53]	$Pr_{0.6}Ba_{0.4}Fe_{0.8}Cu_{0.2}O_{3-\delta}$	Air, H_2O	$Ce_{0.8}Gd_{0.2}O_{2-\delta}$-$(Li,Na,K)_2CO_3$	400	1	1.4 V (two-electrodes)	0.385	0.6	0.336 * (acid trap)	Nitrates used in synthesis Ammonia used in synthesis Acid trap used No blank test	no
Amar et al. (2014)[54]	$La_{0.6}Sr_{0.4}Fe_{0.8}Cu_{0.2}O_{3-\delta}$-$Ce_{0.8}Gd_{0.18}Ca_{0.02}O_{2-\delta}$	N_2, H_2O	$Ce_{0.8}Gd_{0.18}Ca_{0.02}O_{2-\delta}$-$(Li/Na/K)_2CO_3$	400	1	1.4 V (two-electrodes)	0.18	0.1	0.06 * (acid trap)	Nitrates used in synthesis Ammonia used in synthesis Acid trap used No blank test	no
Amar et al. (2015)[55]	Co_3Mo_3N with Ag	N_2, H_2	$LiAlO_2$-$(Li,Na,K)_2CO_3$	450	1	0.8 V (two-electrodes)	1.18	2.95	1.57 * (acid trap)	Nitrates used in synthesis Ammonia used in synthesis Acid trap used No blank test	no
Cui et al. (2017)[56]	Fe_2O_3/AC (stainless steel electrode)	N_2, H_2O	Molten NaOH/KOH	250	1	1.55 V	29.8	4.9	-	Nitrate used in synthesis Acid trap used No catalyst blank test	no

Ambient conditions were noted as 25 °C and 1 atm. No reported TOF.
* denotes calculated (or estimated) concentrations from parameters given in the papers.

Extended Data Table 3 | Electrochemical N_2 reduction to ammonia in non-aqueous electrolyte

Reference	Catalyst	Reactant	Electrolyte	T (°C)	P (atm)	E(V)	Rate (μmol h^{-1} cm^{-2})	FE (%)	C_{NH3} (ppm)	Comment	^{15}N
van Tamelen et al. (1968)[57]	Titanium complex (Pt electrode)	N_2	Titanium tetraisopropoxide, aluminum chloride in 1,2-dimethoxyethane	-	1	90 V (two-electrodes)	-	-	851 *	Ar blank test, No catatalyst blank test	no
Becker et al. (1987)[58]	Cp_2TiCl_2 (Pt electrode)	N_2	0.3 M n-tetrabutylammonium perchlorate in THF	25	1	-2.05 V vs SCE	-	0.28	-	Acid trap used Ammonium used as an electrolyte ($n\text{-}Bu_4NClO_4$)	no
Tsuneto et al. (1993)[13]	Li (on metal electrode, Ag)	N_2	0.2 M $LiClO_4$ 1 vol% EtOH in THF	25	1	-	2.09	8.4	1.65 *	Ar blank test	no
Tsuneto et al. (1994)[24]	Li (on metal electrode, Fe)	N_2	0.2 M $LiClO_4$+0.18M EtOH in THF	25	50	~ -4 V vs Ag/AgCl/AgCl(sat)	14.34	57.7	-	Ar blank test	no
Köleli et al. (2006)[59]	Polyaniline	N_2	30 mM H_2SO_4 + 0.1M $LiClO_4$ in MeOH	25	49.3	-0.12 V vs NHE	0.16	16.3	0.443 *	Ar blank test Aniline in catalyst	no
Kim et al. (2016)[60]	Ni	N_2, H_2O	10 mM H_2SO_4 in 2-propanol/H_2O (9:1, v/v)	25	1	3.7 V (two-electrodes)	0.0554	0.89	0.126 *	No blank test	no
Kim et al. (2016)[29]	Ni	N_2, H_2O	0.1 M LiCl in ethylenediamine (EDA)	25	1	1.8 V (two-electrodes)	0.129	17.2	-	Neosepta CMX membrane (cation exchange membrane) used Ethylenediamine used as an solvent Ar blank test $^{15}N_2$ test using MS	yes
Zhou et al. (2017)[30]	Fe/FTO Fe/SS	N_2, H_2O	$[P_{6,6,6,14}][eFAP]$ (ionic liquid)	20	1	-0.8 V vs NHE	0.017 0.073	60 45	-	Acid trap used $^{15}N_2$ test using NMR Ar blank test Open circuit blank test	yes

Ambient conditions were noted as 25 °C and 1 atm. No reported TOF.
* denotes calculated (or estimated) concentrations from parameters given in the papers.

Extended Data Table 4 | Photochemical N_2 reduction to ammonia in non-aqueous electrolyte

Reference	Catalyst	Reactant	Electrolyte	Source	Bandgap (eV)	Rate (μmol h^{-1} mg^{-1})	TOF (s^{-1})	C_{NH3} (ppm)	Comment	^{15}N
Zhu et al. (2013)[61]	Hydrogen terminated diamond	N_2	H_2O	High pressure HgXe lamp, λ > 190 nm	5.5	~ 0.64 * μmol h^{-1} cm^{-2} illuminated			Ar control Dark control IR spectra of NH_3 isotopes	Yes
Dong et al. (2015)[62]	Nitrogen vacancies on graphitic carbon nitride (g-C_3N_4)	N_2	Aqueous 20% Methanol	300 W Xe lamp, λ > 420 nm	2.74	1.24		~ 41 * (2.4 mM)	Ar control Dark control N containing electrode UV-vis Nessler's reagent LCMS of indophenol	Yes
Banerjee et al. (2015)[63]	FeMoS-Chalcogels	N_2	Aqueous pyridinium hydrochloride and sodium ascorbate	150 W Xe lamp		0.03 *	3.1×10^{-5} *	5.21	Dark control Ar control Control without proton or electron source NMR and LCMS of indophenol	Yes
Li et al. (2017)[64]	Layered bismuth oxyhalides	N_2	H_2O	Visible light	2.81	104.2			Ar control With and without oxygen vacancies control	No
Liu et al (2016) [65]	FeMoS-FeS-SnS chalcogel	N_2	Aqeuous PyrH and NaAc	Xenon lamp λ > 190 nm	0.7		4.7×10^{-5} *	16	Dark control, NMR	Yes
Hu et al. (2017)[66]	Cu doped g-C_3N_4	N_2	DI water, Ethanol	High pressure Na lamp 400-800 nm	2.56	0.264 * (8.8 mg L^{-1} g_{cat}^{-1} h^{-1})		70.4 * (352 mg/L)	UV-vis Nessler's reagent LCMS on indophenol No blank tests No Argon control	Yes
Hirakawa et al. (2017)[67]	Surface oxygen vacancies on TiO_2	N_2	H_2O	High pressure Hg lamp λ > 280 nm		7.6×10^{-4} *	2.9×10^{-6} *	~ 3 * (175.9 μM)	Argon control Dark control Nessler's reagent LCMS on indophenol	Yes

Values in blue color are calculated (or estimated) with given values in the papers. Ambient conditions were 25°C and 1 atm.
* denotes calculated (or estimated) rate and concentration from parameters given in the papers.